Electronic Supplementary Material (ESI) for Journal of Materials Chemistry B.

Supporting information

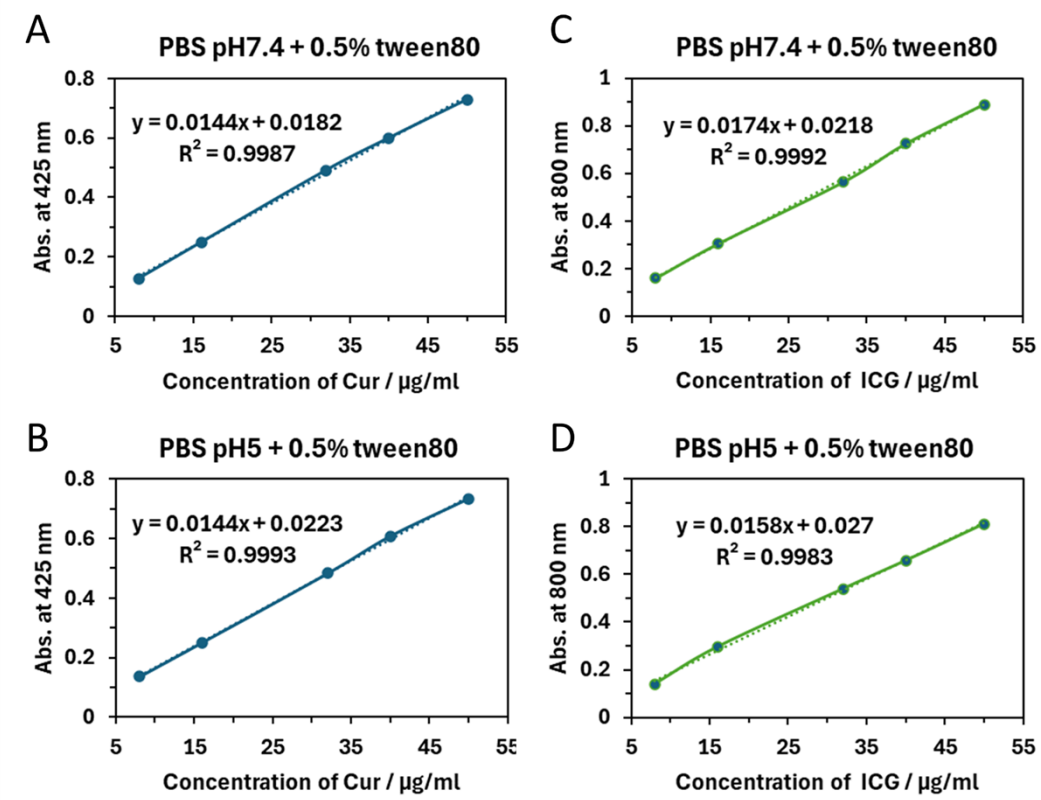

Figure S1. The calibration curves of (**A, B**) Cur and (**C, D**) ICG in PBS buffers at pH 7.4 and pH 5.0 with 0.5% Tween80. The curves plot the linear relationships between the absorbance of agents (Abs. of Cur at 425 nm, and Abs. of ICG at 800 nm) and their concentrations.

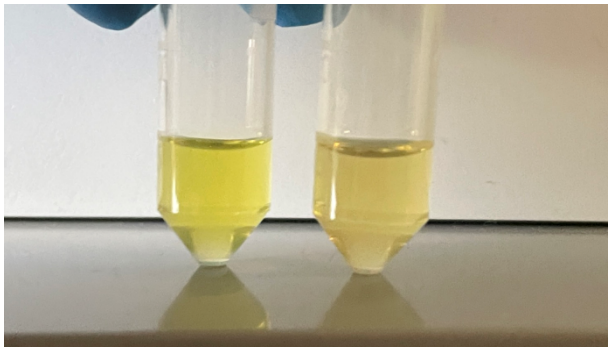

Figure S2. The diluted aqueous suspensions of ICG-Cur/thin MPN (left) and ICG-Cur/thick MPN (right) NPs.

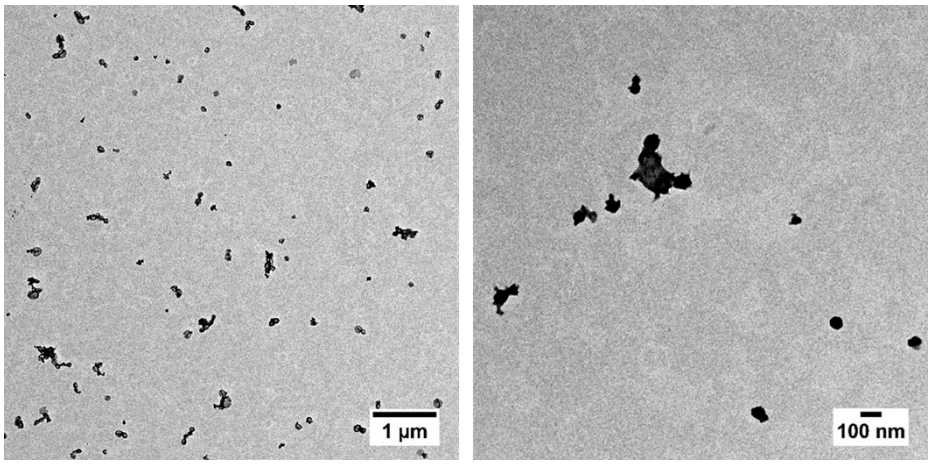

Figure S3. ICG-Cur/thick MPN NPs form some small aggregates observed by zoom-out TEM images.

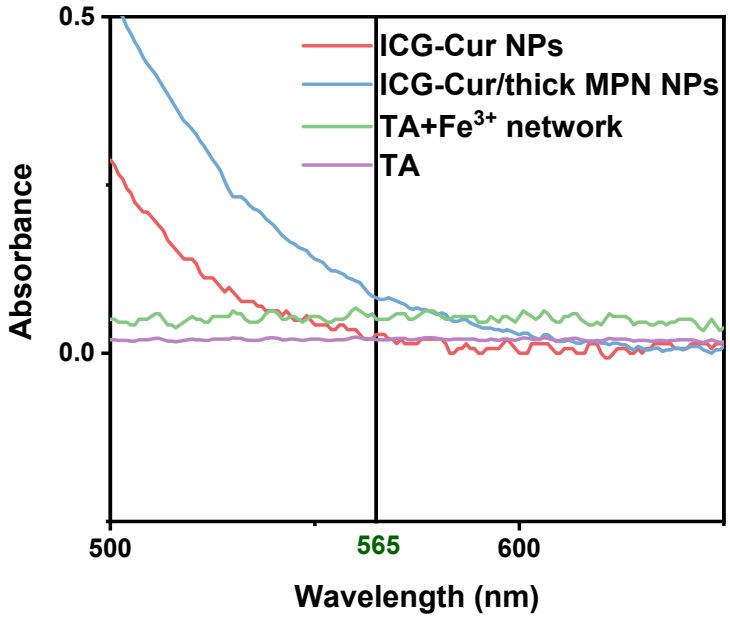

Figure S4. A zoom-in graph of UV-Vis spectra of ICG-Cur NPs and ICG-Cur/thick MPN NPs.

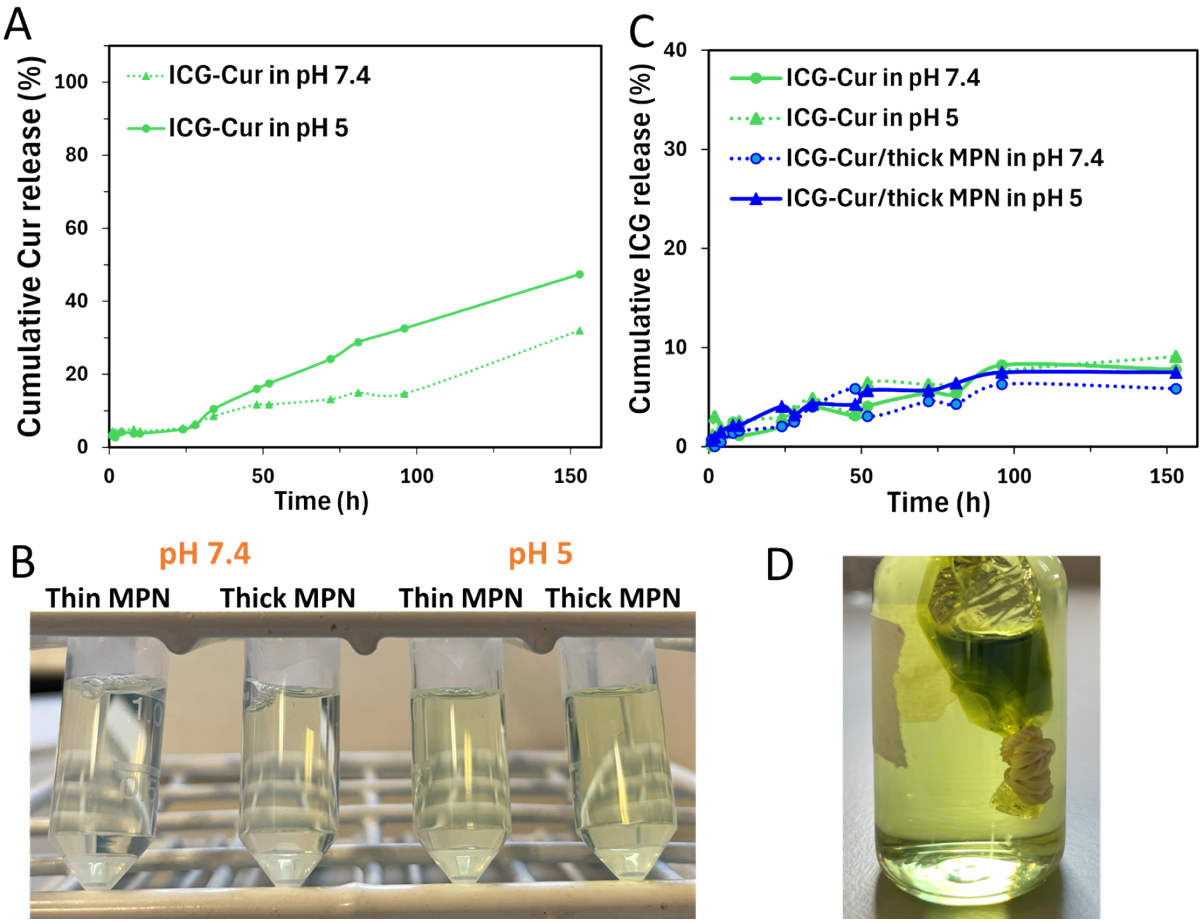

Figure S5. The drug release study of NPs. (**A**) Cumulative Cur release curves of ICG-Cur NPs at pH = 7.4 and 5. (**B**) Photos show the 1 mL release mediums of ICG-Cur/thin MPN and ICG-Cur/thick MPN NPs at pH 7.4 and 5 conditions, respectively, after 69 h of release. At pH 7.4, both NPs exhibit low drug release, as indicated by the colourless and transparent release media. Thick MPN NPs show the most yellow release medium at pH 5, indicating the highest Cur release among four groups. (**C**) Cumulative ICG release curves of ICG-Cur NPs and ICG-Cur/thick MPN NPs at pH = 7.4 and 5. (**D**) The photo displays the drug release of ICG-Cur/thick MPN NPs after 150 h of release. Only the yellow Cur molecules are released from NPs. The color of the NPs change back to green (the color of ICG molecules) from brown (Figure S2) and are trapped in the dialysis bag.

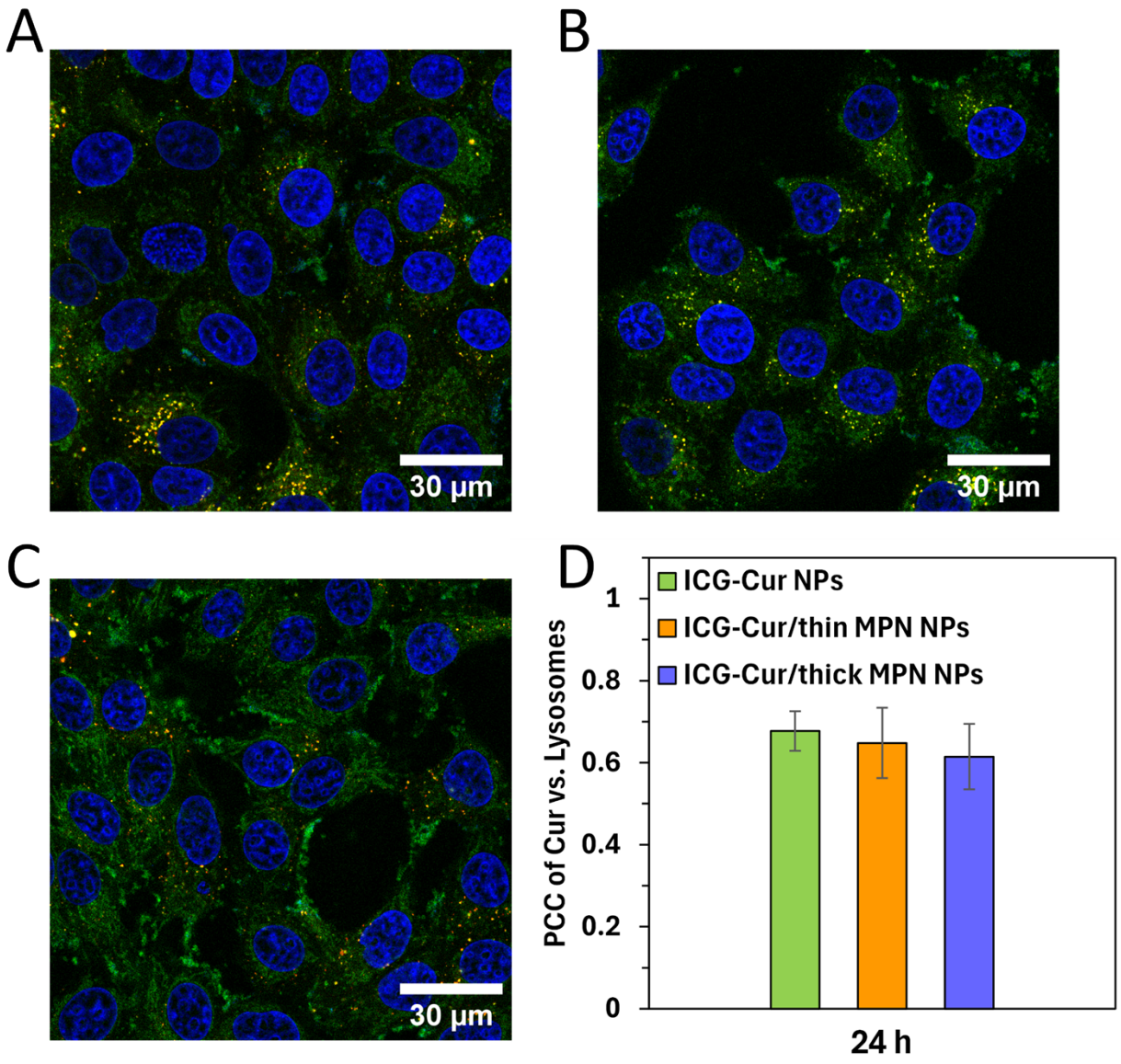

Figure S6. Endo/lysosomal escape of (A) ICG-Cur NPs, (B) ICG-Cur/thin MPN NPs and (C) ICG-Cur/thick MPN NPs after 24 h of coincubation with MCF-7 cells. Nuclei (blue fluorescence) were stained by Hoechst 33342, and lysosomes (red fluorescence) were stained by LysoTracker red. Green fluorescence is from Cur in NPs. Scale bars = 30 μm. (**D**) Calculated Pearson's correlation coefficient (PCC) values of corresponding NPs vs endo/lysosomes at 24 h. Data represent mean values ± standard deviation (n > 50). All three groups show an increased PCC values above 0.5 because the lysosomes disrupted by the NPs can no longer be specifically stained.

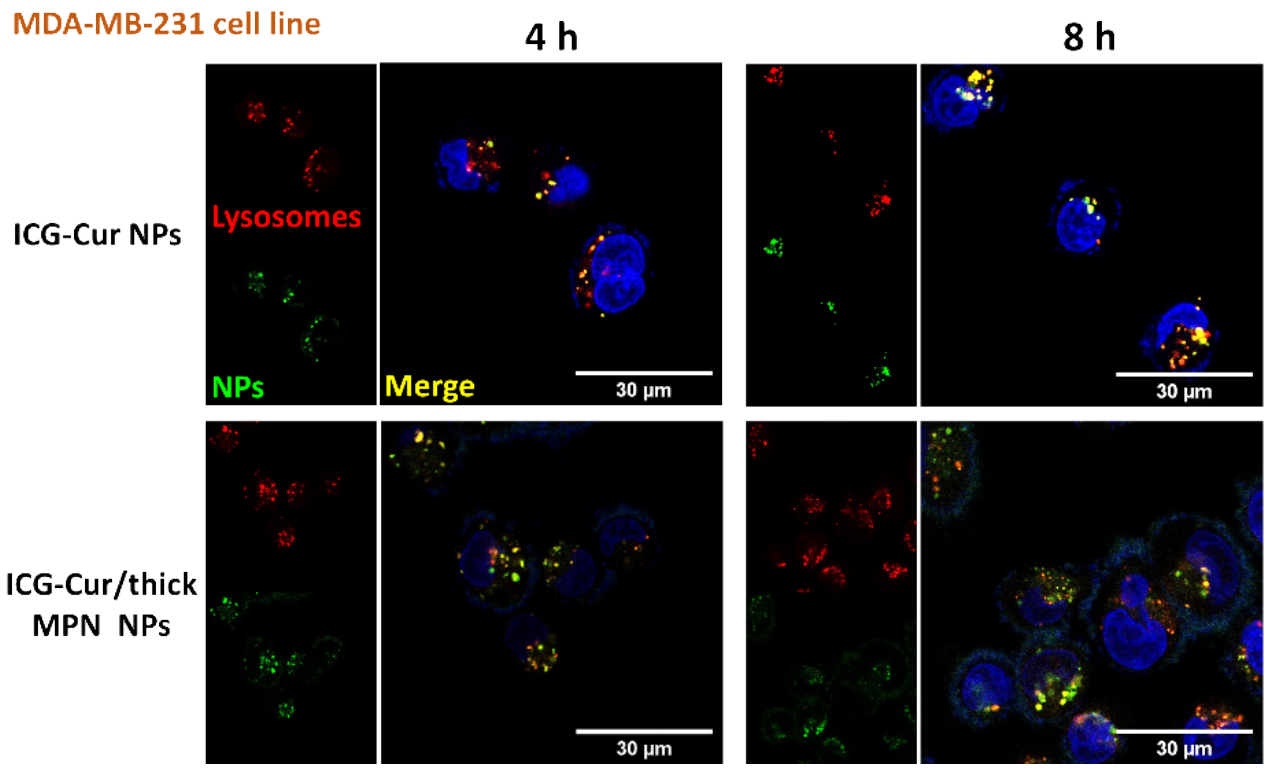

Figure S7. Endo/lysosomal escape of NPs in MDA-MB-231 cell line. CLSM images of MDA-MB-231 cells incubated with ICG-Cur NPs and ICG-Cur/thick MPN NPs at incubation times of 4 h and 8 h. Nuclei (blue fluorescence) were stained by Hoechst 33342, and lysosomes (red fluorescence) were stained by LysoTracker red. Green fluorescence is from Cur in NPs. Scale bars = 30 μm.

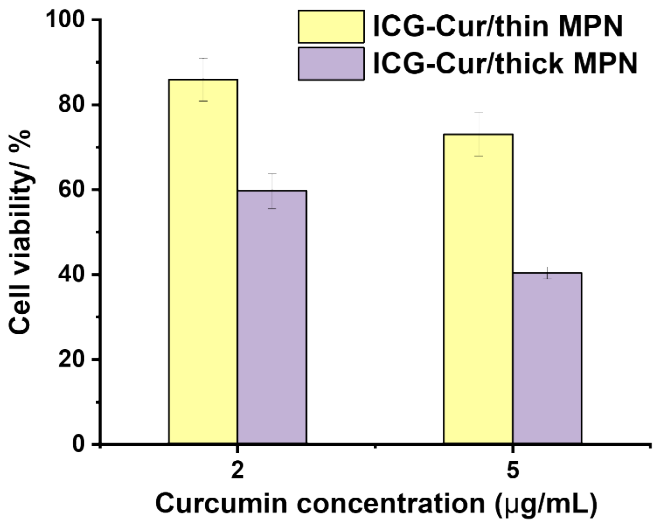

Figure S8. Cell viabilities of MDA-MB-231 cells after being incubated with ICG-Cur/ thin MPN NPs and ICG-Cur/ thick MPN NPs for 48 h.

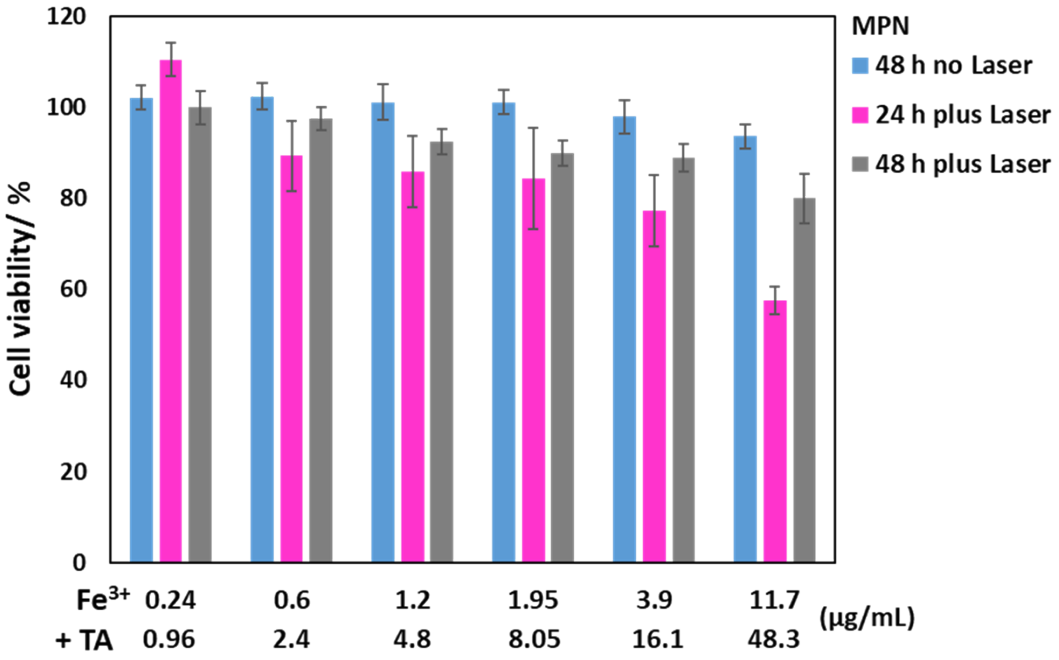

Figure S9. The cytotoxicity of MPN to MCF-7 cells in the absence or presence of laser irradiation was assessed by the CCK-8 viability assay. Fe^{3+} and TA were pre-mixed in the culture medium to form MPN complexes with different concentrations before being applied to cells (Fe^{3+}/TA concentrations ranging from 0.24/0.96 to 11.7/48.3 μg/mL). For no laser

groups, the cells were co-incubated with MPN for 48 h without the laser treatment. For plus laser groups, the cells were first co-incubated with MNP for 8 h, then irradiated with an 808 nm laser at 1.5 W/cm^2 for 3 min. After irradiation, the cells were further incubated with MPN for additional 16 h or 40 h, resulting a total co-incubation time of 24 h (24 h plus Laser) or 48 h (48 h plus Laser). Data represent the mean value of measurements conducted in quadruplicate ± standard deviation.

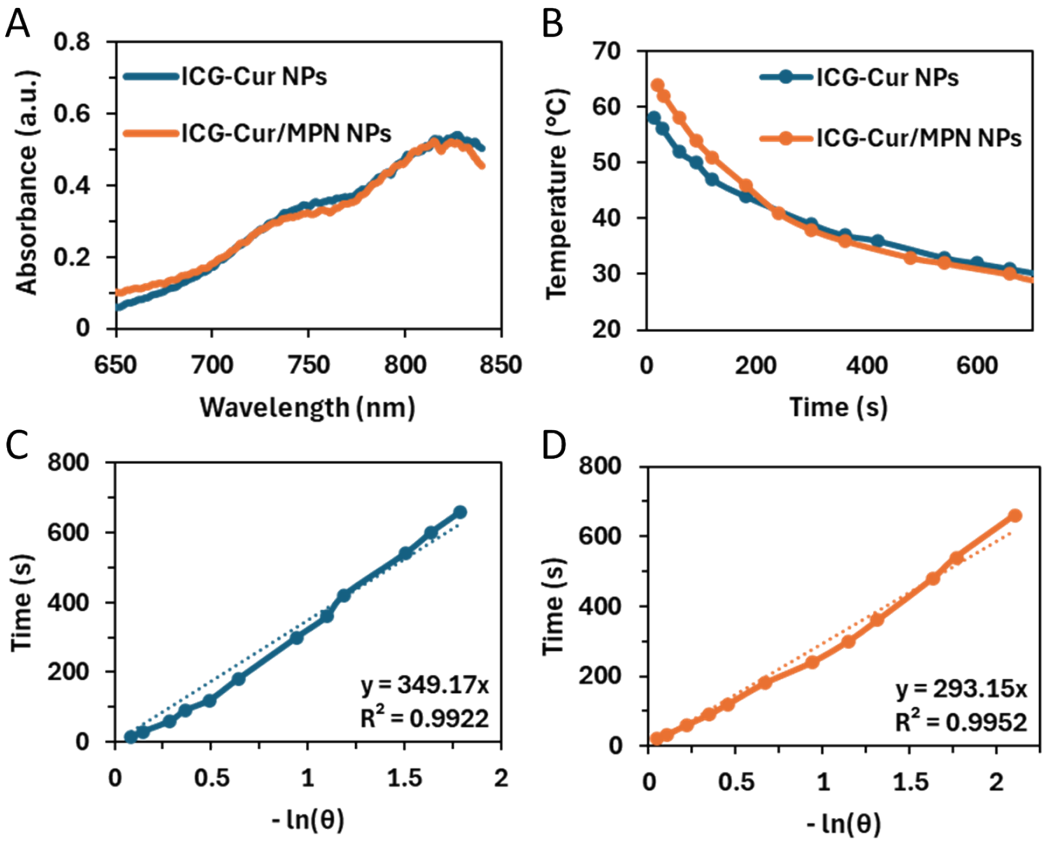

Figure S10. Photophysical properties of ICG-Cur NPs and ICG-Cur/thick MPN NPs (at 40 μg/mL ICG concentration). (A) Absorption spectra of water-dispersible NPs from 650 nm to 850 nm. (B) The temperature changes of NPs in aqueous dispersion after the laser irradiation was turned off (cooling stage). Plot of the cooling time versus negative natural logarithm of a dimensionless parameter (- ln(θ)) obtained from the cooling curve of ICG-Cur NPs (C) and ICG-Cur/thick MPN NPs (D) in (B).

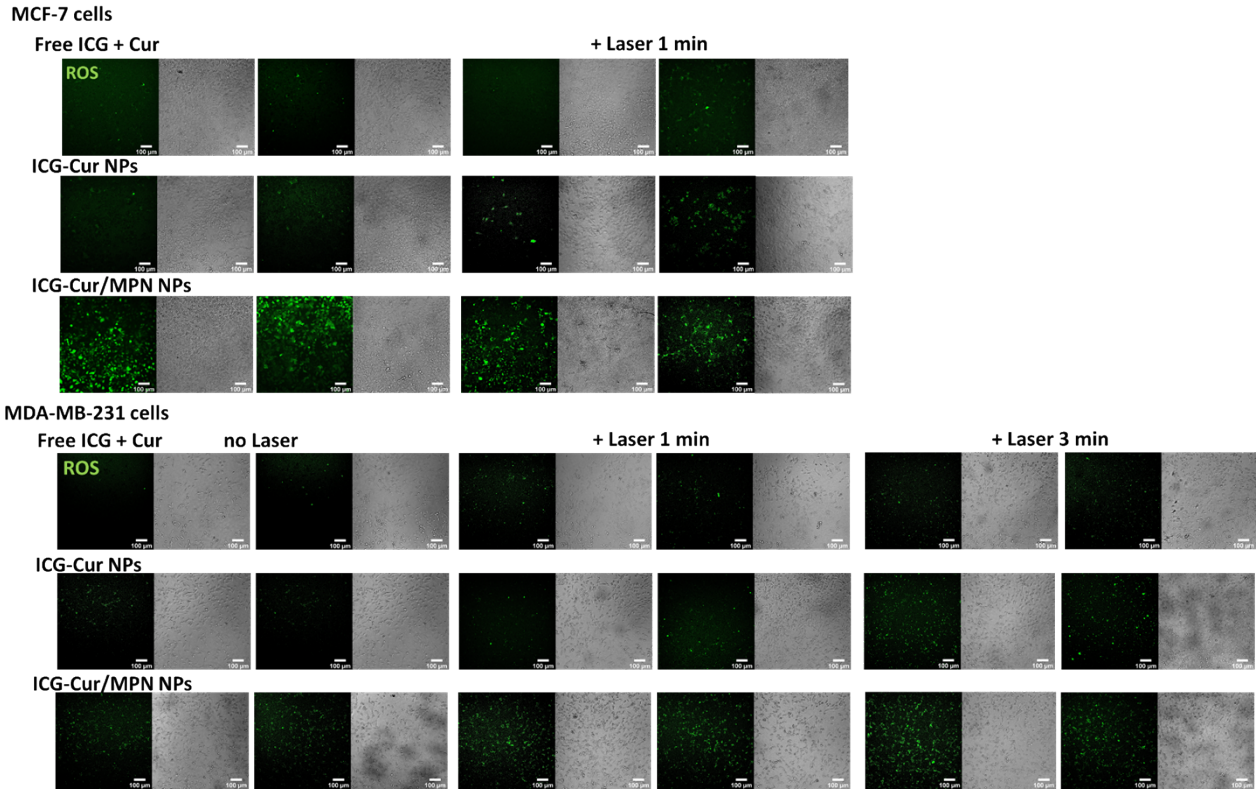

Figure S11. Fluorescent images of ROS generation (green fluorescence) of different samples (the two more repeated groups for each condition) in MCF-7 and MDA-MB-231 tumor cells, in the absence and presence of 1.0 W/cm^2 808 nm laser irradiation. Scale bars = 100 μm.

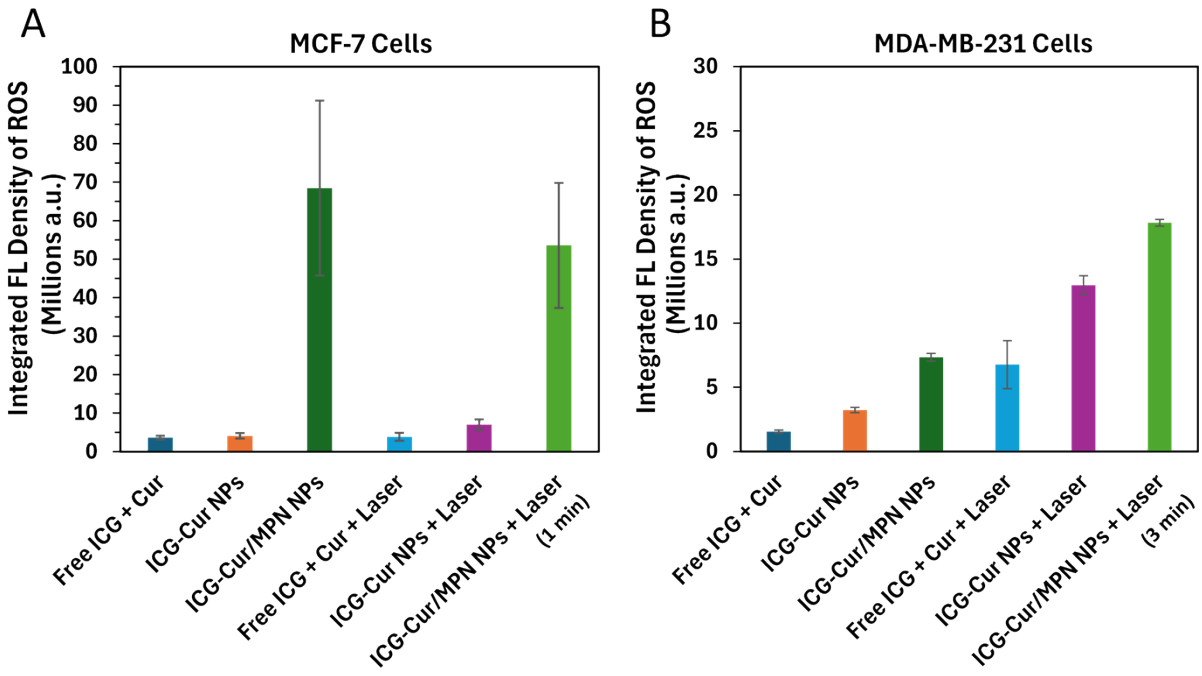

Figure S12. Quantitative analysis of ROS generation in cancer cells. The values of integrated fluorescence densities from DCFH-DA signals in MCF-7 cells (A) and MDA-MB-231 cells (B) were obtained from the measurement of three fluorescent images (Figures 4B & S11) for each treatment group by Image J software. Data are expressed as mean ± standard deviation.

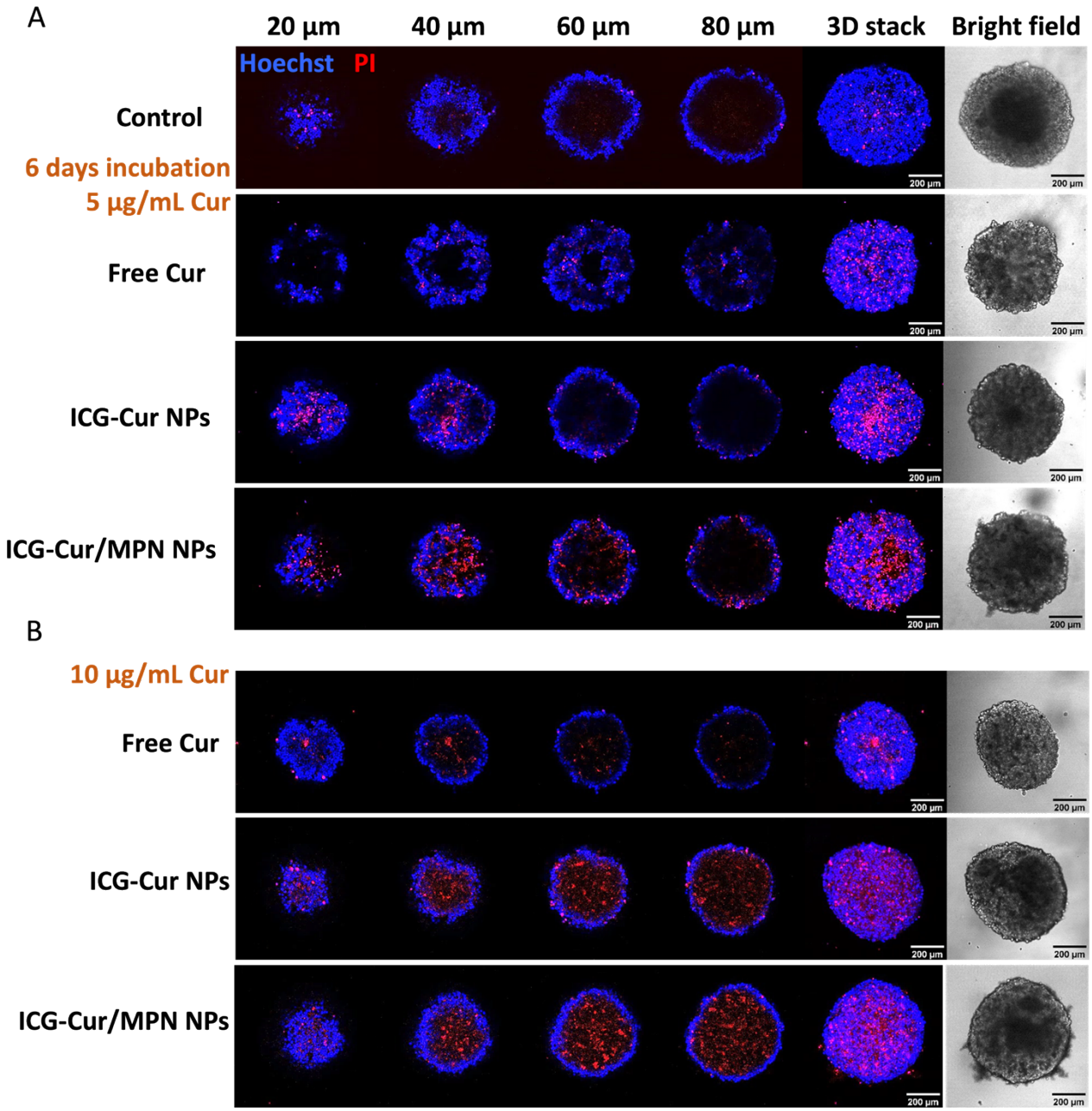

Figure S13. Cytotoxicity of free Cur, ICG-Cur NPs, and ICG-Cur/MPN NPs for 3D MCF-7 breast cancer spheroids. Cell spheroids were costained with Hoechst 33342 (blue fluorescence) and PI (red fluorescence) to indicate live and apoptosis/necrosis cells. Bright-field and fluorescence images of different transverse sections (depth increases with 20 µm) and reconstructed 3D stacks (0 – 150 µm) of cell spheroids after incubation with agents at the concentration of Cur is 5 µg/mL for 6 days (**A**), and 10 µg/mL for 6 days (**B**). Scale bars = 200 µm.

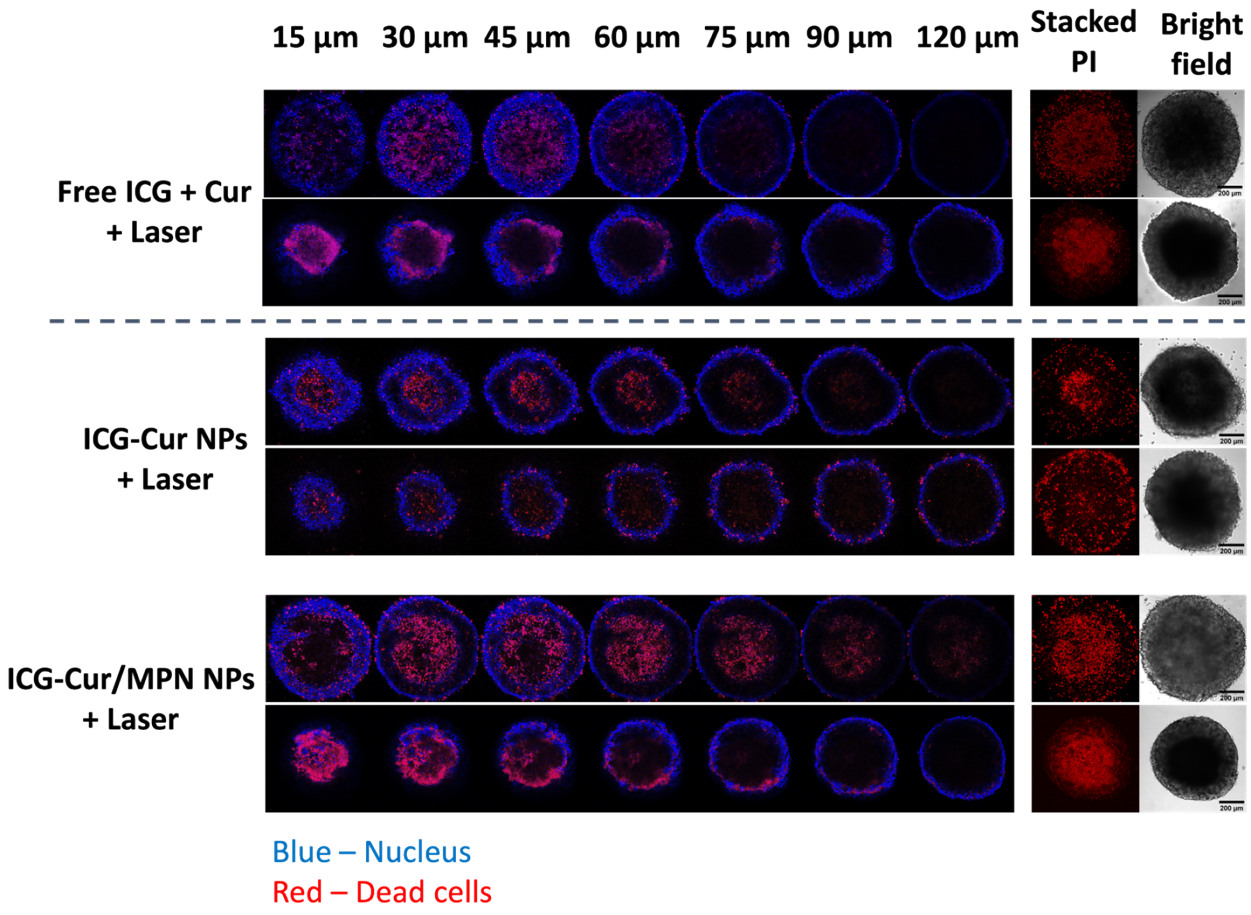

Figure S14. Cytotoxicity of free ICG + Cur, ICG-Cur NPs, and ICG-Cur/MPN NPs (the concentration of Cur is 5 µg/mL) for 3D MCF-7 breast cancer spheroids (two repeated spheroids for each condition) under the 808 nm laser irradiation at the power density at of 1.5 W cm^{-1} for 3 min. Cell spheroids were costained with Hoechst 33342 (blue fluorescence) and PI (red fluorescence) to indicate live and apoptosis/necrosis cells, respectively. Fluorescence images of different transverse sections (depth increases with 15 µm) and reconstructed 3D stacks of PI channel of cell spheroids (0 – 150 µm). Scale bars = 200 µm.

ICG-Cur/thin MPN	ICG-Cur/thick MPN		MPN Composition	
At Cur concentration (μg/mL)		Corresponding concentration of ferric iron and TA in their MPN layers →	Fe^{3+} (μg/mL)	TA (μg/mL)
2			0.24	0.96
5			0.6	2.4
10			1.2	4.8
	5		1.95	8.05
28	10		3.9	16.1
	30		11.7	48.3

Table S1. Calculation of the mass of Fe^{3+} and TA in MPN for the thin or thick MPN coated ICG-Cur NPs at different drug concentrations.